



This is a repository copy of *Control of ferromagnetic properties of Ni₈₀Fe₂₀ thin films by voltage-induced oxidation.*

White Rose Research Online URL for this paper:
<http://eprints.whiterose.ac.uk/135854/>

Version: Accepted Version

Article:

Wood, J.M., Oseghale, C.I. orcid.org/0000-0002-4404-7850, Cespedes, O. et al. (2 more authors) (2018) Control of ferromagnetic properties of Ni₈₀Fe₂₀ thin films by voltage-induced oxidation. *Journal of Applied Physics*, 124 (8). 085304. ISSN 0021-8979

<https://doi.org/10.1063/1.5045552>

© 2018 The Authors. This is an author produced version of a paper subsequently published in: *Journal of Applied Physics*, 124, 085304 (2018); <https://doi.org/10.1063/1.5045552>. Uploaded in accordance with the publisher's self-archiving policy.

Reuse

Items deposited in White Rose Research Online are protected by copyright, with all rights reserved unless indicated otherwise. They may be downloaded and/or printed for private study, or other acts as permitted by national copyright laws. The publisher or other rights holders may allow further reproduction and re-use of the full text version. This is indicated by the licence information on the White Rose Research Online record for the item.

Takedown

If you consider content in White Rose Research Online to be in breach of UK law, please notify us by emailing eprints@whiterose.ac.uk including the URL of the record and the reason for the withdrawal request.



eprints@whiterose.ac.uk
<https://eprints.whiterose.ac.uk/>

Control of ferromagnetic properties of Ni₈₀Fe₂₀ thin films by voltage-induced oxidation

J. M. Wood¹, C. I. Oseghale², O. Cespedes³, M. Grell⁴, D. A. Allwood¹

¹Department of Materials Science & Engineering, University of Sheffield, Portobello Street, Sheffield, S1 3JD, UK

²Department of Chemical & Biological Engineering, University of Sheffield, Portobello Street, Sheffield, S1 3JD, UK

³School of Physics and Astronomy, E. C. Stoner Laboratory, University of Leeds, Leeds, LS2 9JT, UK

⁴Department of Physics & Astronomy, University of Sheffield, Hounsfield Road, Sheffield, S3 7RH, UK

Abstract

We demonstrate large voltage-induced changes of magnetic properties in thin films of Ni₈₀Fe₂₀ (permalloy) when gated using an ionic liquid medium (1-ethyl-3-methylimidazolium bis(trifluoromethylsulfonyl)imide (EMIMTFSI)). The coercivity and magnetic moment of 5 nm thick permalloy films could be reduced by 75% and 35% respectively, by using applied voltages. These changes were partially restored by reversing the potential polarity. Electrochemical, time-course magnetometry and surface analysis measurements suggest that the voltage-induced changes are due to changes in the oxidation state at the surface of the film causing a thinning of the permalloy layer. The control of soft magnetic properties with low voltages may be of use in tuneable devices.

1. Introduction

Active control of magnetic properties offers significant flexibility in devices such as memories and sensors. This has been demonstrated in multiferroic¹⁻⁴, piezoelectric-magnetostrictive composite⁵⁻⁷, ferromagnetic semiconductor⁸⁻¹⁰ and magnetic thin film¹¹⁻¹⁸ systems. The latter cases showed that it is possible to control ferromagnetic properties with voltage or electric field directly. Maruyama et al.¹⁷ demonstrated voltage control of magnetic anisotropy of Fe monolayers by using a polyimide/MgO bilayer as a dielectric material to create electric fields at the magnetic interface. Applying voltages of ± 200 V caused a 39% change in the surface anisotropy, with negative voltages inducing a perpendicular magnetic anisotropy (PMA) in the film. This was attributed to a change in the occupancy of 3d electrons in the Fe adjacent to the MgO. Bauer et al.¹² showed that oxygen migration across a PMA GdO_x/Co interface could be controlled using voltage and heat treatments. This resulted in a significant drop in coercivity and entire loss of PMA after applying -4 V to the oxide layer, and complete reversibility after applying +4 V and heating to 100 °C. Again these effects were attributed to a change in magnetic anisotropy due to the oxygen ion presence. Electrolytes have also been used as an alternative to oxide dielectrics. Weisheit et al.¹¹ added Na⁺ ions to propylene carbonate to generate electric fields of up to 4 GV.m⁻¹ at the interface with FePt and FePd films. This induced changes of up to 4.5% in coercivity, attributed to a change in unpaired 3d electrons at the interface. Di et al.¹⁹ used an electrochemical approach to vary the surface chemistry of a thin film of Co in aqueous KOH solution to achieve reversible voltage-induced changes in coercivity, magnetization and surface anisotropy. The recent focus on using ionic liquids to create high electric fields at the magnetic interface has resulted in relatively low ($< \pm 5$ V) applied voltages creating large changes in coercivity and

magnetization of Fe, Ni and Co films¹³⁻¹⁵, which has again been attributed to control of oxidation conditions.

Permalloy ($\text{Ni}_{80}\text{Fe}_{20}$) is a popular material for use in thin films²⁰ and patterned structures^{21,22}. Here we demonstrate direct voltage control of coercivity and magnetic moment in permalloy thin films when part of an electrochemical cell made with the ionic liquid 1-ethyl-3-methylimidazolium bis(trifluoromethylsulfonyl)imide (EMIMTFSI). These changes in coercivity remained after voltage was removed, which shows a non-volatile change in the surface.

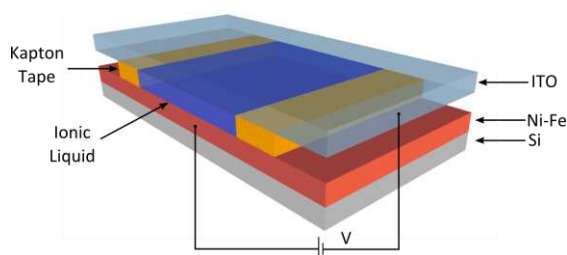


Figure 1. Schematic of experimental cell consisting of a 5 nm thermally evaporated $\text{Ni}_{80}\text{Fe}_{20}$ film on Si substrate with the ionic liquid (EMIMTFSI) enclosed by two strips of Kapton® tape and an ITO-coated glass slide. Voltage is applied across the cell by electrical connections to the permalloy film and ITO-coated glass.

2. Method

Thin films of permalloy ($\text{Ni}_{80}\text{Fe}_{20}$) were thermally evaporated at a base pressure of 1×10^{-7} mbar onto a Si (100) substrate containing a native oxide. Sample dimensions were approximately 1 cm x 2 cm laterally and 5 nm in thickness, verified by atomic force microscopy (AFM; Veeco Nanoscope 3D Dimension 3100). The measurement cell (Fig. 1) consisted of two strips of Kapton® tape, 10 mm x 2 mm x 0.03 mm, placed onto the magnetic film to create an insulating barrier. 10-20 μL of EMIMTFSI (IOLITEC, 99%) was deposited between the Kapton strips using a syringe. EMIMTFSI was used as the ionic liquid because it has a large electrochemical window (ECW) of approximately 4.4 V²³, which allows a wide range of voltages to be applied, and is known to be stable in air.²³ A transparent indium tin oxide (ITO)-coated glass slide was placed over the assembly with the ITO contacting the ionic liquid to ensure optical access to the permalloy film.

Voltage was applied using the permalloy and ITO layers as electrodes, with the potential of the permalloy defined relative to the ITO. This created an electric double layer (EDL) at the magnetic film/ionic liquid interface generating a large electric field.²⁴ Magnetic hysteresis loops of the $\text{Ni}_{80}\text{Fe}_{20}$ films were obtained using longitudinal magneto-optical Kerr effect (MOKE) magnetometry, with 632 nm wavelength laser light. The coercivity, H_C , and switching behavior were obtained from hysteresis loops measured at a frequency of 6 Hz averaged over 500 loops (i.e. taking approximately 80 s overall). The cell was then dismantled and the thin films washed in isopropanol alcohol (IPA) to stabilize the surface against further action by the ionic liquid. Vibrating sample magnetometry (VSM; Quantum Design MPMS 3) was used to characterize the magnetic moment of the washed films. X-ray photoelectron spectroscopy (XPS; Thermo K-alpha) analyzed the surface properties of the washed thin films using 1486.6 eV X-ray beams with a 400 μm spot size and an electron pass energy of 200 eV. XPS measurements were made at room temperature in three positions on each sample and averaged. Cyclic voltammetry (CV) (Solartron Analytical 1400-1470E) was performed on cells consisting of two permalloy-coated Cu disks separated by the ionic liquid. Cyclic voltammograms were recorded by sweeping the potential in the anodic direction from

the open-circuit potential to +2.5 V and then in the cathodic direction to -2.5 V and back to the starting potential, at a scan rate of 5 mV.s⁻¹.

3. Results

Before exploring magnetic effects it was important to establish the electrochemical nature of permalloy. Figure 2 shows a CV loop obtained using potentials between +2.5V and -2.5 V until a stabilized CV characteristic was observed. The CV characteristic shows three anodic and three cathodic peak current densities: the first and primary anodic peak (oxidation reaction) appeared at +0.30 V with $J = 0.234 \text{ mA.cm}^{-2}$ (peak a); this was followed by two oxidation peaks at +1.76 V and +1.95 V (peaks b and c, respectively). In the reverse scan direction (reduction reaction), the three (negative-going) peaks appeared at +2.25 V, -0.23 V and -1.81 V (peaks d, e and f, respectively). The increased current density in the forward scan direction is due to the oxidation at the interface between the 1-ethyl-3-methylimidazolium [EMIM] group and the permalloy film, while the increase in current density on the reverse scan is due to reduction of the interfacial species created in the forward scan.²⁵ The ECW of EMIMTFSI is the potential range where there is no oxidation or reduction, i.e. inert within this potential range (defined here as where the absolute current density, $|J|$ does not exceed 1 mA.cm⁻²) and was calculated by subtracting the reduction potential limit from oxidation potential limit.^{23,25,26} The value of 4.4 V obtained for the ECW width here is in agreement with previous measurements.^{23,25} In a further CV study where the applied voltage was only cycled between positive voltages and 0V (no negative voltages) the current peak at +2.6V was only present in the first cycle, which indicated a saturation of the oxidation process.

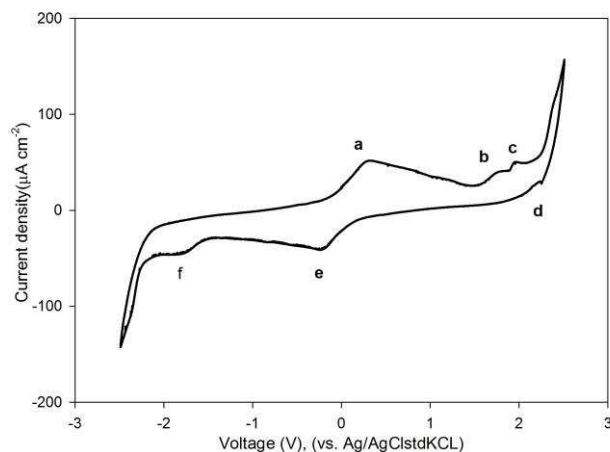


Figure 2. Cyclic voltammogram of a Cu-permalloy-EMIMTFSI-permalloy-Cu cell between +2.5 V and -2.5 V, against a silver chloride reference electrode. a)-f) identify significant peaks in current density passing through the cell.

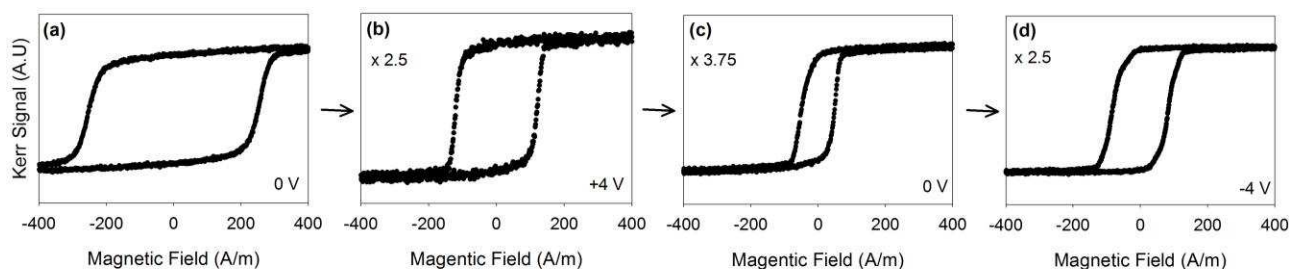


Figure 3. MOKE-generated hysteresis loops of 5nm permalloy film inside permalloy-EMIMTFSI-ITO cell under a sequence of voltages (a) 0 V, (b) +4 V, (c) 0 V, (d) -4 V. Parts (b)-(d) also show the degree of signal enlargement applied to the data (compared to part (a)) for presentation purposes

Magnetic hysteresis loops were taken from a single sample under a sequence of applied voltages of 0 V, +4 V, 0 V and -4 V, with each applied for approximately 5 minutes before a hysteresis loop was obtained at each voltage. Hysteresis loops showed a significant decrease in coercivity when the voltage was increased to +4 V (Fig. 3a and b), while also showing a 2.5 times decrease in Kerr signal. The coercivity and Kerr signal decreased further when the voltage was decreased to 0 V (the coercivity by 80% in Fig. 3c compared to original value). When subsequently applying -4 V (Fig. 3d), the coercivity increased by 59% of the minimum value at 0 V (Fig 3c). At -4 V the Kerr signal returned to a comparable value to that of +4 V. The simultaneous observed changes in coercivity and Kerr signal suggest a decrease in thickness of the ferromagnetic film.

Measurements were repeated on fresh samples with smaller steps of 1 V up to a maximum positive voltage value of +3 V. Each voltage was applied for 2 minutes before the MOKE measurement was performed, apart from -4 V which was followed by MOKE measurements after 2, 4, 6 and 10 minutes. The voltage was then removed and the samples washed in IPA to stabilize the surface against further action by the ionic liquid before another MOKE measurement. The current through the cell was measured every 10 s throughout to give simultaneous cyclic voltammetry and MOKE magnetometry. Figure 4a shows similar results to Fig 3, with a decrease in coercivity of over 70% on application of +3 V. The increase in measured current (Fig. 4b) at +3 V indicates an oxidative effect on the film, also demonstrated by CV plots in Fig 2. On reversal of the voltage from +2 V to -2 V there is little change in the coercivity and current, indicating that there is little chemical change. Application of -3 V saw a small increase in negative-going current and a slight increase in coercivity (Fig. 4a). These effects increased upon application of -4 V and suggest a chemical reduction of the film. Maintaining the voltage at -4 V for a total of 10 minutes increased the coercivity to within 13% of its original value.

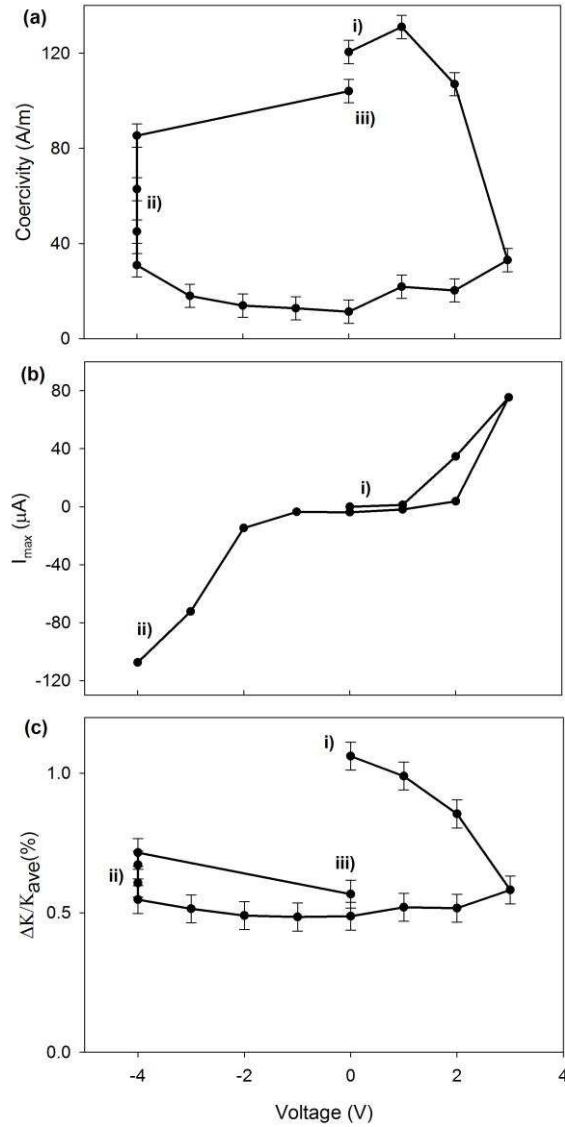


Figure 4. (a) Coercivity of 5nm permalloy film within a permalloy/EMIMTFSI/ITO cell as a function of voltage. (b) Maximum current passing through permalloy/EMIMTFSI/ITO cell at different applied voltages. (c) Fractional Kerr signal, $\Delta K/K_{ave}$, of 5nm permalloy film as a function of voltage, while part of a permalloy/EMIMTFSI/ITO cell. i) Denotes the start of the voltage sequence, 0V. ii) The cell remained for 10 minutes at -4 V and with measurements made at 2, 4, 6 and 10 minutes. iii) The cell was dismantled, the permalloy film washed in IPA and a final measurement made (so not shown in part (b)).

The MOKE hysteresis loops used to obtain coercivity in Fig. 4a were further analyzed to obtain the fractional Kerr signal $\Delta K/K_{ave}$, where ΔK and K_{ave} are the difference in Kerr signal and average Kerr signal in each loop, respectively. For the film thicknesses relevant here, $\Delta K/K_{ave}$ is proportional to changes in relative magnetic moment.²⁷ Figure 4c shows that $\Delta K/K_{ave}$ follows a similar trend as coercivity to changes in applied voltage, decreasing with the initial increasing positive voltage and then increasing again as the voltage polarity is reversed. The similarity of change in $\Delta K/K_{ave}$ and coercivity is less strong following application of -4 V (Fig. 4a and b), with $\Delta K/K_{ave}$ only reaching approximately 50% of its initial value when returned to 0V.

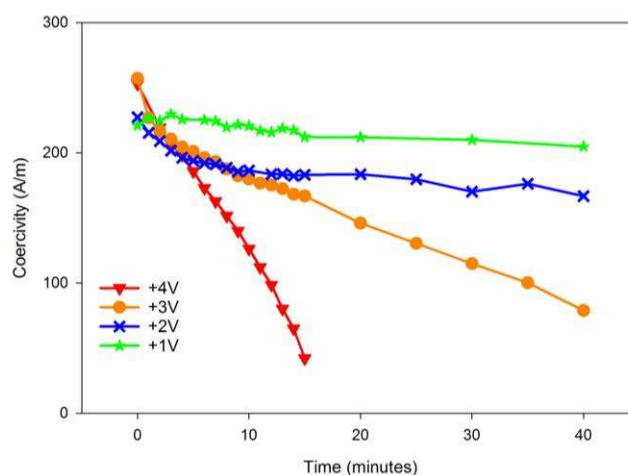


Figure 5. Time course coercivity measurements of 5 nm permalloy films obtained from MOKE hysteresis loops, while exposed to +1 V, +2 V, +3 V and +4 V, as part of permalloy/EMIMTFSI/ITO cell.

The non-volatile nature of these voltage-dependent changes in coercivity and $\Delta K/K_{ave}$ suggest the changes are due to redox reactions, as seen in previous similar studies of other materials^{12,28}. The kinetics of the oxidation were investigated by performing MOKE magnetometry measurements under +1V, +2V, +3V and +4V with hysteresis loops obtained at regular intervals. Figure 5 shows that the coercivity decreased at a higher rate for larger voltages, indicating faster oxidation. This means exposure time can also be used as a technique to control coercivity. However, the coercivity change is not a simple function of voltage and reflects the non-linear nature of electrochemistry present, as seen in the cyclic voltammogram in Figure 2.

Thin films that had been subject to different voltages for 5 minutes and washed in IPA were characterized magnetically by VSM. All the samples that had a negative voltage applied were previously exposed to +3 V for 5 minutes. Figure 6a demonstrates a decrease in magnetic moment per unit area for increasing positive voltage up to +3 V. The magnetic moment per unit area continued to decrease upon reversing voltage polarity up until -4 V where the magnetic moment increased (Fig 6b). The coercivity measured from Figure 6a & 6b showed a 60% decrease at +3 V and a subsequent increase at -4 V, following the same trend as MOKE coercivity (Fig. 3 & 4). It should be noted that the switching fields measured by VSM are less precise than MOKE in this study.

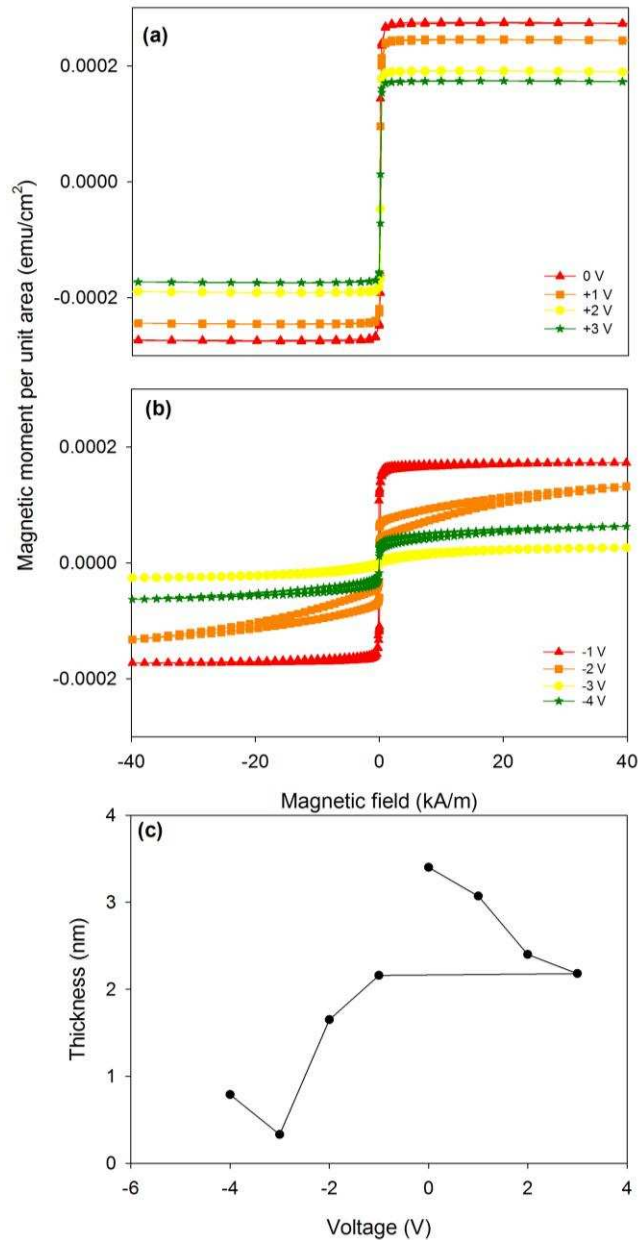


Figure 6. VSM generated hysteresis loops showing magnetic moment per unit area of permalloy film as a function of applied field after exposure to a sequence of voltages while part of a permalloy/EMIMTFSI/ITO cell; all cells were dismantled and all films washed in IPA prior to VSM characterization. The voltage sequence passed from (a) 0 V to +3 V and subsequently to (b) -4V; all negative voltages had prior exposure to +3 V for 5 minutes. The reason for the different loop shape for the -2 V sample is unclear but does not affect the measurement of magnetic moment. (c) Reduced permalloy film thickness with applied voltage, calculated from reduced magnetic moment for 5 nm permalloy films observed in VSM data.

Calculation of magnetic moment per unit volume using a nominal initial film thickness of 5 nm produced reduced saturation magnetization values (M_S) for permalloy, even for unexposed samples, for which $M_S = 550$ kA/m was obtained. This could reflect a reduced thickness of ferromagnetic permalloy in the film due to native oxidation.²⁹ Calculation of the ferromagnetic thickness using $M_S = 800$ kA/m for permalloy³⁰ gave an initial ferromagnetic thickness of 3.4 nm. This correlates well with the observation of Fitzsommons et al of a 1.5 nm thick native oxide layer in permalloy films.²⁹ Figure 6c shows the variation of ferromagnetic thickness with applied voltage, demonstrating a decrease in film thickness with

increasing voltage until -4 V was applied, when the ferromagnetic film thickness increased again. These voltage-induced magnetic layer thickness changes provide a simple explanation of the changes in MOKE measurements discussed above.

Thin films that had been subject to a voltage for 5 minutes and washed in IPA were analyzed using XPS, which probes 5-10 nm from the surface. All samples that had a negative voltage applied were previously exposed to +3 V for 5 minutes. The peak parameters for all spectra were fitted using data from Biesinger et al.^{31,32} Figure 7a shows an example oxygen 1s energy peak from a permalloy film that had not been exposed to an applied voltage, following background subtraction and peak calibration to the C 1s peak. Deconvolution of the oxygen peak (Fig. 7a) shows components attributed to lattice oxides (529.5 eV), which are characteristic of permalloy oxidation³³, hydroxide/lattice defects (531.5 eV) and water/organic species (533.7 eV). Fitzsimmons et al.²⁹ suggest that a NiO layer is present on permalloy films that have been exposed to air. Figure 7b shows the oxygen 1s peaks for all samples and Fig. 7c the magnitude of the three peak components, with voltage plotted to follow the sequence in which it was applied. The lattice oxide peak remained unchanged until -3 V and -4 V, where it decreased. However, wide-energy survey spectra showed the appearance of In at -3 V and -4 V, thus covering the film and reducing the lattice oxide peak intensity. The water/organic species component decreased after +1 V, which is attributed to the electrolysis of water generating hydroxide ions. This is further supported by the increase in hydroxide/defect lattice oxide components, shift in peak position and the minor peak at +0.3 V shown in CV data in Figure 2.

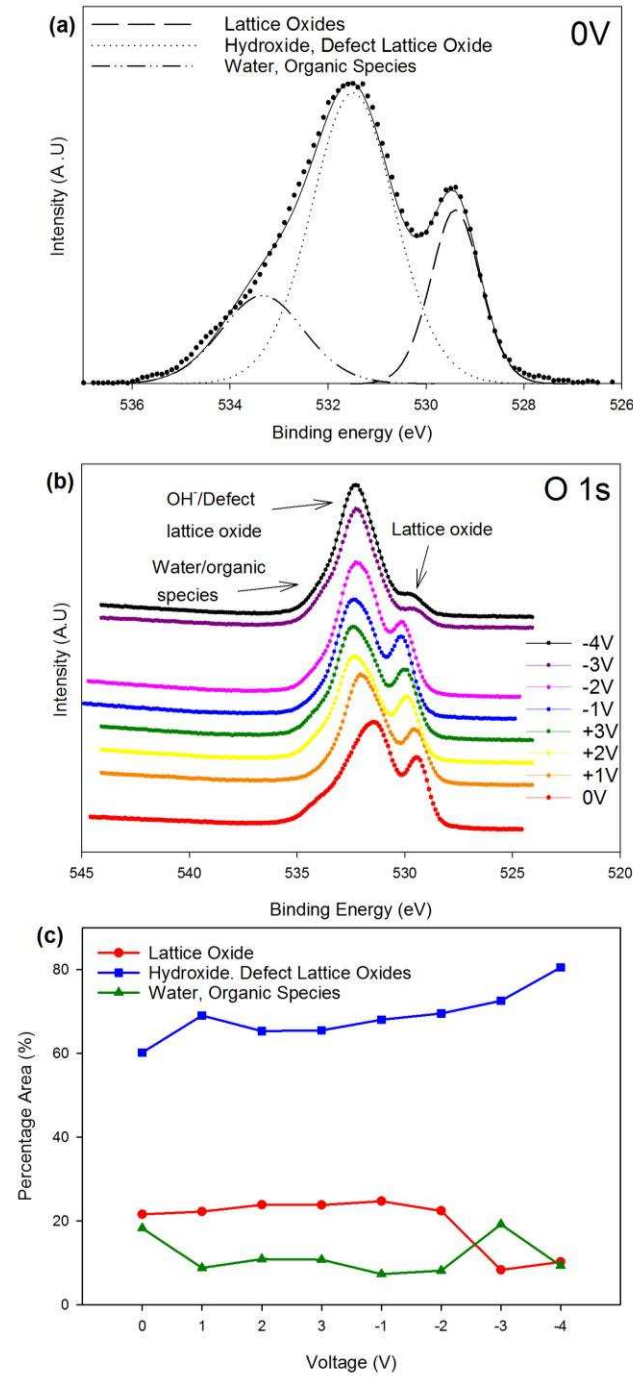


Figure 7. (a) Deconvoluted XPS spectrum for O 1s energy range at 0 V (b) XPS spectra for O 1s spectra for voltage range 0 V to +3 V to -4 V, arrows indicating lattice oxide species, hydroxide/defect lattice oxides and water/organic species, spectra have here been offset (c) change in percentage area of O 1s components as a function of voltage.

Figure 8 shows the XPS data for the Ni 2p energy range, including example peak deconvolution of XPS for the 0 V Ni sample (Fig. 8a). Fitting parameters from Biesinger et al.³² were again used along with a Shirley background offset³². The sharp peak at 862.6 eV is attributed to Ni metal in the permalloy while secondary peaks are attributed to NiO, NiFe₂O₄ and Ni(OH)₂ (Fig. 8a), further demonstrating the presence of an oxide layer above the permalloy at 0 V. Figure 8b and 8c shows a decrease in the Ni metal peak with increasing

positive voltage, while the Ni oxide and hydroxide peak grow, further suggesting a thinning of the Ni metal layer as voltage increases.

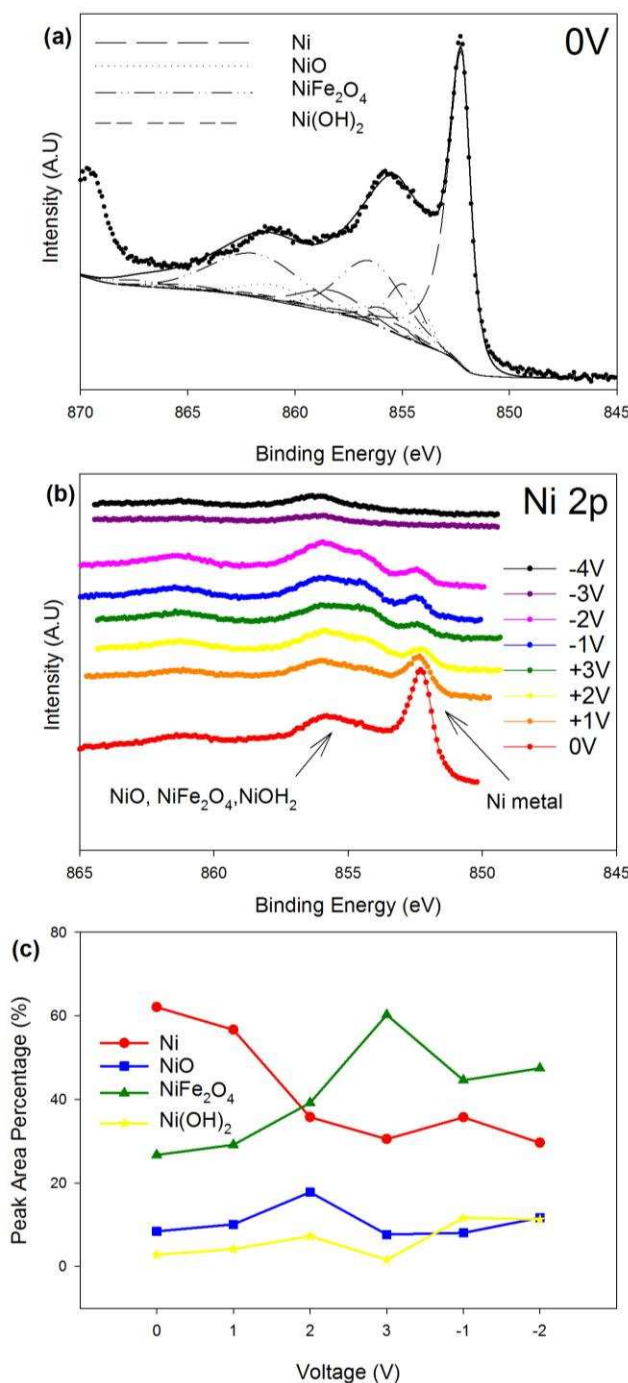


Figure 8. (a) Deconvoluted XPS spectrum for Ni 2p energy range at 0 V (b) XPS spectra for Ni 2p spectra for voltage range 0 V to +3 V to -4 V, arrows indicating Ni metal peak and oxides/hydroxides, spectra have here been offset (c) change in percentage area of Ni 2p components as a function of voltage.

Figure 9 shows the XPS spectra for the Fe 2p energy range, including deconvolution of the peak for the 0 V sample (Fig. 9a) and identification of contributions from Fe metal and NiFe₂O₄. No metal Fe peak was observed for samples above +2 V (Fig. 9b and 9c), with subsequent spectra showing only NiFe₂O₄, although In may again have masked any metal Fe in the -3 V and -4 V samples.

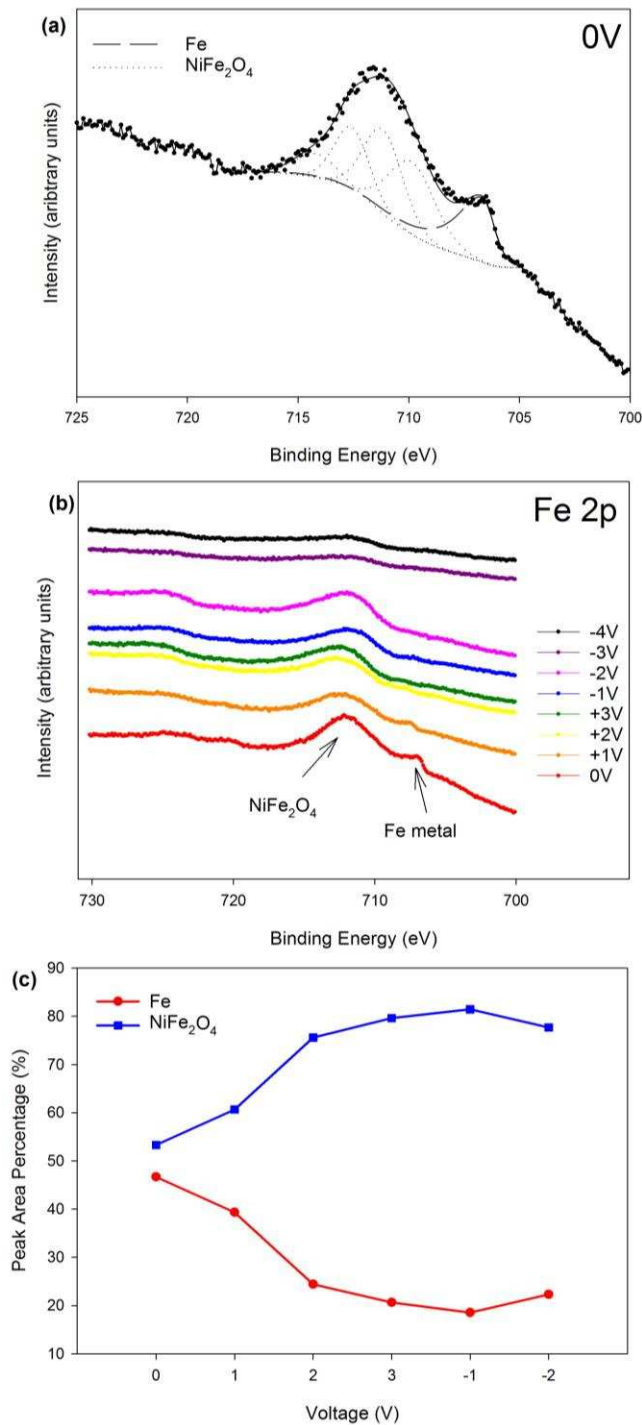


Figure 9. (a) Deconvoluted XPS spectrum for Fe 2p energy range at 0 V (b) XPS spectra for Fe 2p spectra for voltage range 0 V to +3 V to -4 V, arrows indicating Fe metal peak and NiFe₂O₄, spectra have here been offset (c) change in percentage area of Fe 2p components as a function of voltage.

This agrees well with the observation of Fitzsimmons et al²⁹ of a constant 1.5 nm layer of NiO on the permalloy surface after exposure to air, described above. Further, Fitzsimmons et al show the formation of a 1 nm thick Fe-rich oxide layer directly beneath the NiO that increases in thickness with increasing oxidation. These reports are both consistent with the XPS data shown here. Thus increasing positive voltage increases the thickness of the Fe-rich oxide, effectively thinning the permalloy layer, reducing the coercivity, relative magnetization and magnetic moment.

The changes observed in XPS measurements concur with the cyclic voltammetry in suggesting significant oxidation of permalloy for voltages above +2 V. The resulting variation of ferromagnetic film thickness also explains the reversible changes in magnetic coercivity and magnetic moment observed in both MOKE and VSM data.

4. Summary

Large semi-reversible changes in coercivity, relative magnetization and magnetic moment of permalloy thin films as part of an electrochemical cell containing the ionic liquid, EMIMTFSI, were observed upon application of voltage across the cell. XPS and cyclic voltammetry both showed that increasing positive voltages increased the degree of oxidation in the films. These increases in oxidation explain the observed changes in magnetic properties, due to changes in the thickness of the metallic permalloy. The rate of decrease in coercivity also increased with larger voltages, consistent with electrochemical processes. When a negative voltage is applied the effect is reversed and the magnetic properties recovered substantially. The simple arrangement afforded by the electrolytic mediation of applied voltage offers flexibility in future tuneable magnetic structures. Future experiments could incorporate heat treatments¹² or wider exploration of voltage sequences and exposure times to improve the reversibility of magnetic properties.

Acknowledgements

The authors would like to thank the team at the National EPSRC XPS Users' Service (NEXUS) for carrying out the XPS measurements and acknowledge EPSRC for a PhD studentship (grant EP/I000933/1).

References

- ¹ Y. Tokunaga, Y. Taguchi, T. Arima, and Y. Tokura, *Nat. Phys.* **8**, 838 (2012).
- ² J.T. Heron, M. Trassin, K. Ashraf, M. Gajek, Q. He, S.Y. Yang, D.E. Nikonov, Y.H. Chu, S. Salahuddin, and R. Ramesh, *Phys. Rev. Lett.* **107**, 1 (2011).
- ³ D. Lebeugle, a. Mougín, M. Viret, D. Colson, and L. Ranno, *Phys. Rev. Lett.* **103**, 2 (2009).
- ⁴ S.M. Wu, S.A. Cybart, P. Yu, M.D. Rossell, J.X. Zhang, R. Ramesh, and R.C. Dynes, *Nat. Mater.* **9**, 756 (2010).
- ⁵ J.W. Lee, S.C. Shin, and S.K. Kim, *Appl. Phys. Lett.* **82**, 2458 (2003).
- ⁶ N. Lei, T. Devolder, G. Agnus, P. Aubert, L. Daniel, J.-V. Kim, W. Zhao, T. Trypiniotis, R.P. Cowburn, C. Chappert, D. Ravelosona, and P. Lecoeur, *Nat. Commun.* **4**, 1378 (2013).
- ⁷ C. Thiele, K. Dörr, O. Bilani, J. Rödel, and L. Schultz, *Phys. Rev. B* **75**, 054408 (2007).

- ⁸ D. Chiba, F. Matsukura, and H. Ohno, *Appl. Phys. Lett.* **89**, 2004 (2006).
- ⁹ D. Chiba, M. Yamanouchi, F. Matsukura, and H. Ohno, *Science* **301**, 943 (2003).
- ¹⁰ H. Ohno and H. Ohno, *Nature* **408**, 944 (2000).
- ¹¹ M. Weisheit, S. Fähler, A. Marty, Y. Souche, C. Poinsignon, and D. Givord, *Science* **315**, 349 (2007).
- ¹² U. Bauer, L. Yao, A.J. Tan, P. Agrawal, S. Emori, H.L. Tuller, S. Van Dijken, and G.S.D. Beach, *Nat. Mater.* **14**, 174 (2014).
- ¹³ M. Kawaguchi, K. Shimamura, S. Ono, S. Fukami, F. Matsukura, H. Ohno, D. Chiba, and T. Ono, *Appl. Phys. Express* **5**, 6 (2012).
- ¹⁴ Y.N. Yan, X.J. Zhou, F. Li, B. Cui, Y.Y. Wang, G.Y. Wang, F. Pan, and C. Song, *Appl. Phys. Lett.* **107**, (2015).
- ¹⁵ K. Shimamura, D. Chiba, S. Ono, S. Fukami, N. Ishiwata, M. Kawaguchi, K. Kobayashi, and T. Ono, *Appl. Phys. Lett.* **100**, (2012).
- ¹⁶ M. Jiang, X.Z. Chen, X.J. Zhou, B. Cui, Y.N. Yan, H.Q. Wu, F. Pan, and C. Song, *Appl. Phys. Lett.* **108**, 202404 (2016).
- ¹⁷ T. Maruyama, Y. Shiota, T. Nozaki, K. Ohta, N. Toda, M. Mizuguchi, a a Tulapurkar, T. Shinjo, M. Shiraishi, S. Mizukami, Y. Ando, and Y. Suzuki, *Nat. Nanotechnol.* **4**, 158 (2009).
- ¹⁸ X. Zhou, Y. Yan, M. Jiang, B. Cui, F. Pan, and C. Song, *J. Phys. Chem. C* **120**, 1633 (2016).
- ¹⁹ N. Di, J. Kubal, Z. Zeng, J. Greeley, F. Maroun, and P. Allongue, *Appl. Phys. Lett.* **106**, 122405 (2015).
- ²⁰ S.S.P. and S.C.S. Stoecklein, W, *Phys. Rev. B* **38**, 6847 (1988).
- ²¹ D. Atkinson, D. a Allwood, G. Xiong, M.D. Cooke, C.C. Faulkner, and R.P. Cowburn, *Nat. Mater.* **2**, 85 (2003).
- ²² R.P.C. D. A. Allwood, G. Xiong, C. C. Faulkner, D. Atkinson, D. Petit, *Science* (80-.).

309, 1688 (2005).

²³ M. Hayyan, F.S. Mjalli, M.A. Hashim, I.M. AlNashef, and T.X. Mei, *J. Ind. Eng. Chem.* **19**, 106 (2013).

²⁴ T. Fujimoto and K. Awaga, *Phys. Chem. Chem. Phys.* **15**, 8983 (2013).

²⁵ T. Liu, R. Vilar, S. Eugénio, J. Grondin, and Y. Danten, *J. Appl. Electrochem.* **45**, 87 (2015).

²⁶ S.P. Ong, O. Andreussi, Y. Wu, N. Marzari, and G. Ceder, *Chem. Mater.* **23**, 2979 (2011).

²⁷ D.A. Allwood, G. Xiong, M.D. Cooke, and R.P. Cowburn, *J. Phys. D Appl. Phys.* **36**, 2175 (2003).

²⁸ C. Bi, Y. Liu, T. Newhouse-Illige, M. Xu, M. Rosales, J.W. Freeland, O. Mryasov, S. Zhang, S.G.E. Te Velthuis, and W.G. Wang, *Phys. Rev. Lett.* **113**, 1 (2014).

²⁹ M. Fitzsimmons, T. Silva, and T. Crawford, *Phys. Rev. B* **73**, 014420 (2006).

³⁰ J.P. Nibarger, R. Lopusnik, Z. Celinski, and T.J. Silva, *Appl. Phys. Lett.* **83**, 93 (2003).

³¹ M.C. Biesinger, B.P. Payne, A.P. Grosvenor, L.W.M. Lau, A.R. Gerson, R. St, and C. Smart, *Appl. Surf. Sci.* **257**, 2717 (2011).

³² M.C. Biesinger, B.P. Payne, L.W.M. Lau, R. St, and C. Smart, 324 (2009).

³³ M. Salou, B. Lescop, S. Rioual, a Lebon, J. Ben Youssef, and B. Rouvellou, *Surf. Sci.* **602**, 2901 (2008).

List of figure captions

Figure 1. Schematic of experimental cell consisting of a 5 nm thermally evaporated Ni₈₀Fe₂₀ film on Si substrate with the ionic liquid (EMIMTFSI) enclosed by two strips of Kapton® tape and an ITO-coated glass slide. Voltage is applied across the cell by electrical connections to the permalloy film and ITO-coated glass.

Figure 2. Cyclic voltammogram of a Cu-permalloy-EMIMTFSI-permalloy-Cu cell between

+2.5 V and -2.5 V, against a silver chloride reference electrode. a)-f) identify significant peaks in current density passing through the cell.

Figure 3. MOKE-generated hysteresis loops of 5nm permalloy film inside permalloy-EMIMTFSI-ITO cell under a sequence of voltages (a) 0 V, (b) +4 V, (c) 0 V, (d) -4 V. Parts (b)-(d) also show the degree of signal enlargement applied to the data (compared to part (a)) for presentation purposes

Figure 4. (a) Coercivity of 5nm permalloy film within a permalloy/EMIMTFSI/ITO cell as a function of voltage. (b) Maximum current passing through permalloy/EMIMTFSI/ITO cell at different applied voltages. (c) Fractional Kerr signal, $\Delta K/K_{ave}$, of 5nm permalloy film as a function of voltage, while part of a permalloy/EMIMTFSI/ITO cell. i) Denotes the start of the voltage sequence, 0V. ii) The cell remained for 10 minutes at -4 V and with measurements made at 2, 4, 6 and 10 minutes. iii) The cell was dismantled, the permalloy film washed in IPA and a final measurement made (so not shown in part (b)).

Figure 5. Time course coercivity measurements of 5 nm permalloy films obtained from MOKE hysteresis loops, while exposed to +1 V, +2 V, +3 V and +4 V, as part of permalloy/EMIMTFSI/ITO cell.

Figure 7. VSM generated hysteresis loops showing magnetic moment per unit area of permalloy film as a function of applied field after exposure to a sequence of voltages while part of a permalloy/EMIMTFSI/ITO cell; all cells were dismantled and all films washed in IPA prior to VSM characterization. The voltage sequence passed from (a) 0 V to +3 V and subsequently to (b)-4V; all negative voltages had prior exposure to +3 V for 5 minutes. The reason for the different loop shape for the -2 V sample is unclear but does not affect the measurement of magnetic moment.(c) Reduced permalloy film thickness with applied voltage, calculated from reduced magnetic moment for 5 nm permalloy films observed in VSM data.

Figure 7. (a) Deconvoluted XPS spectrum for O 1s energy range at 0 V (b) XPS spectra for O 1s spectra for voltage range 0 V to +3 V to -4 V, arrows indicating lattice oxide species, hydroxide/defect lattice oxides and water/organic species, spectra have here been offset (c) change in percentage area of O 1s components as a function of voltage.

Figure 8. (a) Deconvoluted XPS spectrum for Ni 2p energy range at 0 V (b) XPS spectra for Ni 2p spectra for voltage range 0 V to +3 V to -4 V, arrows indicating Ni metal peak and oxides/hydroxides, spectra have here been offset (c) change in percentage area of Ni 2p components as a function of voltage.

Figure 9. (a) Deconvoluted XPS spectrum for Fe 2p energy range at 0 V (b) XPS spectra for Fe 2p spectra for voltage range 0 V to +3 V to -4 V, arrows indicating Fe metal peak and NiFe₂O₄, spectra have here been offset (c) change in percentage area of Fe 2p components as a function of voltage.